



# Interior of nonuniform black strings

Burkhard Kleihaus\*, Jutta Kunz

Institut für Physik, Universität Oldenburg, Postfach 2503 D-26111 Oldenburg, Germany

## ARTICLE INFO

### Article history:

Received 29 November 2007  
Received in revised form 9 May 2008  
Accepted 12 May 2008  
Available online 16 May 2008  
Editor: A. Ringwald

## ABSTRACT

We consider nonuniform black strings inside their event horizon. We present numerical evidence, that the singularity touches the horizon as the horizon topology changing transition is reached.

© 2008 Elsevier B.V. Open access under CC BY license.

## 1. Introduction

Already Kaluza and Klein invoked a fifth dimension to unify gravity and electromagnetism, hiding the higher dimension subsequently by rendering it small and compact. Following these ideas, today supergravity and string theory also put forward the existence of higher dimensions in their attempt to unify the fundamental forces of nature.

In such  $D$ -dimensional manifolds with  $p$  compact dimensions, black holes can either be localized in the compact dimensions, or the black hole horizon can wrap the compact dimensions completely. Black holes which are localized in the compact dimensions have the horizon topology of a  $(D-2)$ -sphere,  $S^{D-2}$ , and are called ‘caged’ black holes [1,2]. In contrast, when the horizon wraps the compact dimensions, the horizon topology reflects the topology of the compact manifold. In the simplest case, the single compact dimension is simply a circle,  $S^1$ . The black holes then have the horizon topology of a torus,  $S^{D-3} \times S^1$ , and are referred to as black strings [1,2].

As long as caged black holes are much smaller than the compact dimension, they resemble more or less  $D$ -dimensional Schwarzschild black holes (when they are static and uncharged). But as their size and with it their mass grows, they begin to feel the finite size of the compact dimension and deform accordingly, reaching a maximal size beyond which they no longer fit into the compact dimension [3,4]. Black strings, on the other hand, exist for all values of the mass. However, as shown by Gregory and Laflamme (GL) [5], such ‘uniform’ black strings (UBS), which do not depend on the compact coordinate, become unstable below a critical value of the mass. GL therefore suggested, that unstable UBS would decay to black holes, which possess higher entropy.

In contrast, Horowitz and Maeda [6] argued that the horizon of UBS could not pinch off in finite affine time. They therefore conjectured that the solutions would settle down to nontranslationally invariant solutions with the same horizon topology as the original configurations, ‘nonuniform’ black strings (NUBS). Shortly after, such NUBS were found perturbatively [7] and numerically [8]. However, the NUBS cannot serve as endpoints of the instability, since they are too massive and possess too low an entropy [7], at least as long as the number of dimensions is smaller than 13 [9], indicating that black holes are the end-state of the instability, nevertheless [1].

Emerging from the UBS branch at the marginally stable solution, the NUBS form a branch of solutions along which the deformation of the horizon along the compact direction perpetually increases. This is illustrated in Fig. 1, where we exhibit the spatial embedding of the horizon of static  $D=6$  black string solutions for a sequence of NUBS, yielding a geometrical view of the increasing nonuniformity of the solutions [10]. We here parametrize the deformation by  $\lambda = \frac{1}{2}(\frac{R_{\max}}{R_{\min}} - 1)$  [7], where  $R_{\max}$  and  $R_{\min}$  represent the maximum and minimum radius of a  $(D-3)$ -sphere on the horizon.

Extrapolating the numerical results to  $\lambda \rightarrow \infty$  shows that the maximal radius  $R_{\max}$  assumes a finite limiting value, while the radius  $R_{\min}$  of the ‘waist’ of the black strings shrinks to zero [4,8,10]. In the limit  $\lambda \rightarrow \infty$ , the horizon will then pinch off, changing the horizon topology from  $S^{D-3} \times S^1$  to  $S^{D-2}$  at a singular ‘merger’ configuration [1,11–13]. Study of the global and horizon properties of NUBS and black holes in  $D=5$  and  $D=6$  dimensions indeed provides persuasive evidence that the NUBS branch merges with the black hole branch at such a topology changing transition [4,10].

A deep question associated with the envisaged transition is whether it is associated with the occurrence of a naked singularity and thus a violation of cosmic censorship. Indeed, it appears possible, that as the black string pinches, a naked singularity is formed, because the singularity, which originally winds the compact dimension, gets broken [1]. To address this question, we here

\* Corresponding author.

E-mail address: kleihaus@theorie.physik.uni-oldenburg.de (B. Kleihaus).

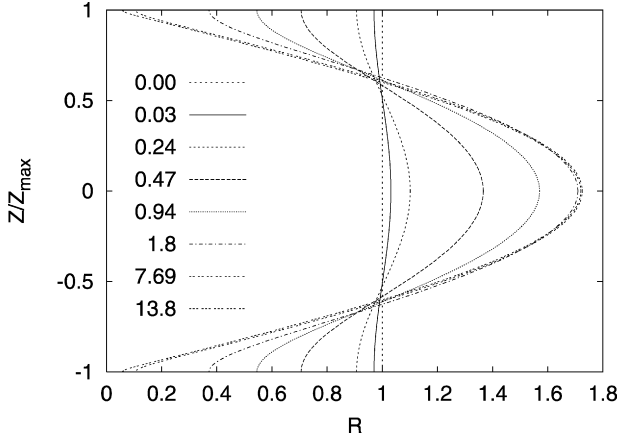


**Fig. 1.** Spatial embedding of the horizon of  $D=6$  black strings with increasing deformation  $\lambda$ , ranging from  $\lambda=0$  to  $\lambda=13.8$ . ( $Z$  denotes the proper length along the compact direction,  $R$  the proper radius of the horizon.)

investigate the inside of nonuniform black strings, to see how the curvature and in particular the singularity evolve, as  $\lambda$  becomes large. Our results indicate, that the singularity will touch the horizon at the topology changing transition.

## 2. Nonuniform black strings

We consider the Einstein action

$$I = \frac{1}{16\pi G} \int_M d^D x \sqrt{-g} R - \frac{1}{8\pi G} \int_{\partial M} d^{D-1} x \sqrt{-h} K, \quad (1)$$

for a  $D$ -dimensional spacetime with one compact direction. We denote the periodic length of the compact direction by  $L$ . Here the last term is the Gibbons–Hawking surface term [14].

A convenient form of the metric is given by [10]

$$ds^2 = -e^{2A} f dt^2 + e^{2B} \left( \frac{d\tilde{r}^2}{f} + dz^2 \right) + e^{2C} \tilde{r}^2 d\Omega_{D-3}^2, \quad (2)$$

where  $z$  is the coordinate of the compact direction.  $A$ ,  $B$ , and  $C$  are functions of  $\tilde{r}$  and  $z$  only, and  $f = 1 - (\tilde{r}_0/\tilde{r})^{D-4}$ . Thus the horizon resides at  $\tilde{r} = \tilde{r}_0$ . The functions  $A$ ,  $B$ , and  $C$  have to be determined from the Einstein equations  $G_t^t = 0$ ,  $G_r^r + G_z^z = 0$  and  $G_\theta^\theta = 0$ . The remaining nontrivial equations  $G_r^{\tilde{r}} - G_z^z = 0$  and  $G_z^{\tilde{r}} = 0$  form the constraints. (For  $A = B = C = 0$  UBS arise.)

We now focus on black strings in  $D=6$  dimensions, since they can be determined with great numerical accuracy up to large deformations [10]. For solutions outside the horizon,  $\tilde{r} \geq \tilde{r}_0$ , we introduce the coordinate  $\tilde{r}$  via  $\tilde{r} = \sqrt{\tilde{r}_0^2 + r^2}$ , while inside the horizon,  $\tilde{r} \leq \tilde{r}_0$ , we define the coordinate  $r$  via  $\tilde{r} = \sqrt{\tilde{r}_0^2 - r^2}$ . In these coordinates the horizon resides at  $\tilde{r} = 0 = r$ . Substitution in the line element Eq. (2) then yields for  $\tilde{r} \leq \tilde{r}_0$

$$ds^2 = e^{2\hat{A}} r^2 dt^2 + e^{2\hat{B}} (-dr^2 + dz^2) + e^{2\hat{C}} d\Omega_3^2, \quad (3)$$

where  $e^{2\hat{A}} = e^{2A}/(\tilde{r}_0^2 - r^2)$ ,  $e^{2\hat{B}} = e^{2B}$ , and  $e^{2\hat{C}} = e^{2C}(\tilde{r}_0^2 - r^2)$ . Inside the horizon the Einstein equations are hyperbolic, the coordinate  $r$  playing the role of ‘time’.

$$\begin{aligned} \hat{A}_{,rr} &= \hat{A}_{,zz} - \frac{\hat{A}_{,r}}{r} - \left( \hat{A}_{,r} + \frac{1}{r} \right) (\hat{A}_{,r} + 3\hat{C}_{,r}) + \hat{A}_{,z} (\hat{A}_{,z} + 3\hat{C}_{,z}), \\ \hat{B}_{,rr} &= \hat{B}_{,zz} + 3\hat{C}_{,r} \left( \hat{A}_{,r} + \frac{1}{r} + \hat{C}_{,r} \right) - 3\hat{C}_{,r} (\hat{A}_{,z} + \hat{C}_{,z}) + 3e^{2(\hat{B}-\hat{C})}, \end{aligned}$$

$$\begin{aligned} \hat{C}_{,rr} &= \hat{C}_{,zz} - \hat{C}_{,r} \left( \hat{A}_{,r} + \frac{1}{r} + 3\hat{C}_{,r} \right) \\ &\quad + \hat{C}_{,z} (\hat{A}_{,z} + 3\hat{C}_{,z}) - 2e^{2(\hat{B}-\hat{C})}. \end{aligned} \quad (4)$$

Initial conditions are given at the horizon (setting  $\tilde{r}_0 = 1$ )

$$\begin{aligned} \hat{A}(0, z) &= A_H(z), \quad \hat{B}(0, z) = B_H(z), \quad \hat{C}(0, z) = C_H(z), \\ \partial_r \hat{A}|_{r=0} &= \partial_r A|_{\tilde{r}=0} = 0, \quad \partial_r \hat{B}|_{r=0} = \partial_r B|_{\tilde{r}=0} = 0, \\ \partial_r \hat{C}|_{r=0} &= \partial_r C|_{\tilde{r}=0} = 0, \end{aligned} \quad (5)$$

where the functions  $A_H(z)$ ,  $B_H(z)$  and  $C_H(z)$  are obtained from the solution outside the horizon. The origin of the  $z$  coordinate is chosen such that  $R_{\min} = e^{C_H(0)}$  and  $R_{\max} = e^{C_H(L/2)}$ .

Setting  $G_t^t = G_r^r + G_z^z = G_{\theta_1}^{\theta_1} = G_{\theta_2}^{\theta_2} = G_\varphi^\varphi = 0$  in the identities  $\nabla_\mu G^{\mu r} = 0$  and  $\nabla_\mu G^{\mu z} = 0$  reveals that the constraints satisfy the advection equations

$$(\partial_r \pm \partial_z)(\sqrt{-g}(G_r^r \mp (G_r^r - G_z^z)/2)) = 0.$$

Consequently, the constraints vanish everywhere, since they vanish at the horizon.

## 3. Numerics

The hyperbolic differential equations (4) are re-written as a set of first order equations in  $r$ . For the evolution in  $r$  we use a fourth order Runge–Kutta method.<sup>1</sup> The ‘spatial’ coordinate is scaled via  $z \rightarrow z/L$ . The difference formulae for  $z$  derivatives are obtained from a polynomial approximation of the functions: If a function  $y$  has values  $y_k$  at the gridpoints  $z_k$ , we approximate the  $q$ th derivative of  $y$  at  $z_k$  by

$$y^{(q)}(z_k) = \sum_{j=k-n}^{k+n} y_j P_{j,k}^{(q)}(z_k). \quad (6)$$

Here  $P_{j,k}^{(q)}(z)$  is the  $q$ th derivative of the Lagrange polynomial of degree  $2n$ ,

$$P_{j,k}(z) = \prod_{\substack{l=k-n \\ l \neq j}}^{k+n} \frac{z - z_l}{z_j - z_l}.$$

To maintain the same order of approximation at all gridpoints we include auxiliary gridpoints  $\{-z_n, -z_{n-1}, \dots, -z_2\}$  and  $\{1+z_1, 1+z_2, \dots, 1+z_n\}$ . The values of the functions at these points are obtained from the symmetry properties  $y(-z) = y(z)$  and  $y(1+z) = y(1-z)$ .

However, if a singularity is encountered at some point  $z_s$ , we have to restrict to the interval  $z_s < z < 1 - z_s$ . In this case the approximation of the  $z$  derivatives is less ‘symmetric’. Thus, if  $z_{k_s}$  is the gridpoint next to  $z_s$ , and  $k_s \leq k < k_s + n$ , we define

$$y^{(q)}(z_k) = \sum_{j=k_s}^{k_s+2n} y_j P_{j,k}^{(q)}(z_k), \quad P_{j,k}(z) = \prod_{\substack{l=k_s \\ l \neq j}}^{k_s+2n} \frac{z - z_l}{z_j - z_l}, \quad (7)$$

and similarly for gridpoints close to  $1 - z_s$ .

As we argue below, the solution becomes singular if  $e^{\hat{C}}$  tends to zero. In order to avoid the singularity we have to restrict to a domain, where  $e^{\hat{C}}$  is larger than some small number, typically  $\approx 10^{-6}$ . Thus the computation is performed in two stages. In the first stage the solution evolves from the horizon ( $r = 0$ ) until it

<sup>1</sup> For the numerical construction of the solutions we have also employed the parameterization  $q(r, z) = e^{-4\hat{A}}$ ,  $w(r, z) = e^{-2(\hat{B}+\hat{C})}$ ,  $\gamma(r, z) = e^{3\hat{C}+\hat{A}}$ .

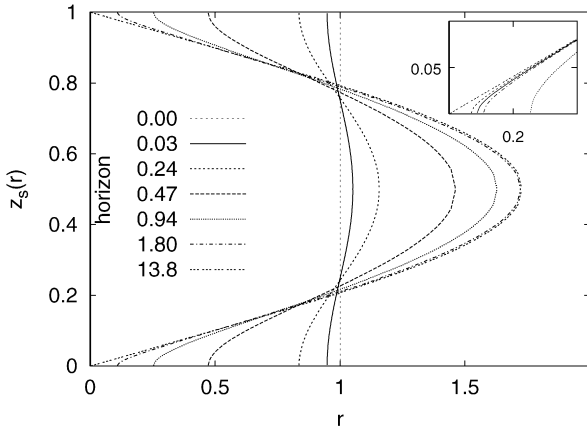


**Fig. 2.** The coordinate  $z_s(r)$  of the location of the singularity is shown for several values of the deformation parameter  $\lambda$  of black strings, ranging from  $\lambda = 0$  to  $\lambda = 13.8$ .

becomes nearly singular at  $z = 0$  and  $z = 1$  for some  $r = r_s$ . During this stage we employ the difference formula (6). In the second stage the solution evolves from  $r = r_s$ . In each Runge–Kutta step we check whether the solution is nearly singular at gridpoints  $z_k$ . If this is the case, we restrict to  $z_{k_s} < z_k < 1 - z_{k_s}$  in the next Runge–Kutta step. During this stage the difference formula (7) is employed. The evolution stops when the  $z$ -interval shrinks to zero.

Typical step sizes used are  $\Delta r \approx 1 - 4 \times 10^{-4}$  and the number of gridpoints ranges between  $N = 100$  and  $N = 2400$ . The order of the difference formula is  $2n = 6 - 14$ . We have checked the consistency of the solutions for different choices of  $\Delta r$ ,  $N$  and  $n$ , and also for different nonequidistant gridpoint distributions.

#### 4. Results

We have constructed NUBS solutions inside their horizon for several values of the deformation parameter  $\lambda$ . Near the horizon the solutions extend smoothly into the interior region. The function  $e^{\hat{C}}$  decreases monotonically for fixed  $z$ . When  $e^{\hat{C}}$  tends to zero at some  $r_s(z)$ , the Kretschmann scalar diverges there, indicating that the curvature singularity resides at  $r_s(z)$ . For UBS the radial coordinate of the singularity is constant,  $r_s(z) = 1$ , while for NUBS with small deformation  $r_s(z)$  shows an oscillation about  $r = 1$  with small amplitude, which then increases with increasing  $\lambda$ . We exhibit the coordinate  $z_s(r)$  of the singularity in Fig. 2 for several values of the deformation parameter  $\lambda$ . (Note the similarity with Fig. 1.)

As seen in the figure, the singularity approaches the horizon at  $z = 0$  and  $z = 1$ , when  $\lambda$  becomes large. This is further demonstrated in Fig. 3, where we exhibit the minimal distance  $R_{\text{sing}} = \int_{r_H}^{r_s} e^{\hat{B}(r,0)} dr$  of the singularity from the horizon at the waist. We note that for large deformation the distance decreases approximately inversely proportional to the deformation,  $R_{\text{sing}} \sim \lambda^{-1}$ . Thus we extrapolate that in the limit  $\lambda \rightarrow \infty$  the singularity will touch the horizon at the waist of the string, i.e., a naked singularity will appear at the topology changing transition [1,12].

We conclude that the deformation of the horizon reflects itself in the location of the singularity. At the symmetric points  $z = 0$  and  $z = 1$ , where the function  $e^{\hat{C}_H}$  yields the minimal horizon radius  $R_{\text{min}}$ , the distance  $R_{\text{sing}}$  of the singularity from the horizon is also minimal. In particular, for large  $\lambda$ ,  $R_{\text{min}} \sim \lambda^{-1}$  along with  $R_{\text{sing}}$  (see Fig. 3). Extrapolating to the limit of infinite deformation, we infer that the singularity touches the horizon at  $z = 0$  and  $z = 1$ , but is hidden well inside the horizon everywhere else.

In order to get further insight into the geometry of space in the NUBS interior, we consider an isometric embedding of surfaces of

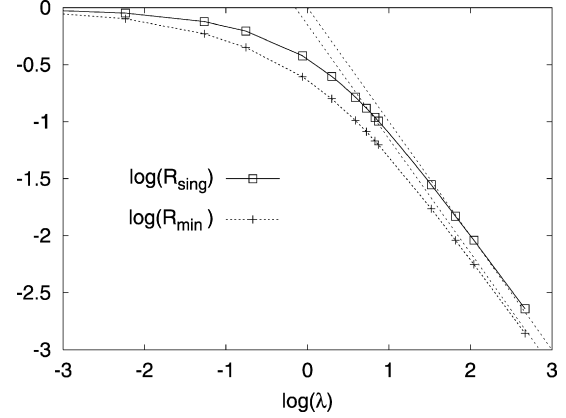


**Fig. 3.** The distance  $R_{\text{sing}}$  from the horizon to the singularity at the waist ( $z = 0$ ) is shown versus the deformation  $\lambda$  for a sequence of NUBS, together with its approximation at large  $\lambda$ ,  $R_{\text{sing}} = \lambda^{-1}$  (dotted). Also shown are the minimal horizon radius  $R_{\text{min}}$  and its asymptote (dotted).

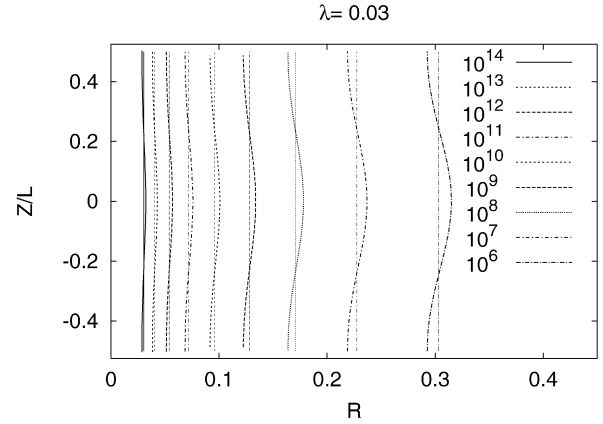


**Fig. 4.** Isometric embedding of surfaces of constant Kretschmann scalar  $K$  for NUBS with  $\lambda = 0.03$ . The straight lines correspond to surfaces of constant  $K$  of UBS with the same temperature.

constant Kretschmann scalar  $K = R_{\mu\nu\rho\sigma} R^{\mu\nu\rho\sigma}$ . Thus, if such a surface has coordinates  $r_K(z), z, \theta_1, \theta_2, \varphi$  (at a fixed time), we define coordinates  $X_i, Z$  by

$$dX_i dX^i + dZ^2 = e^{2\hat{B}} (-(dr_K/dz)^2 + 1) dz^2 + e^{2\hat{C}} d\Omega_3^2 = dR^2 + dZ^2 + R^2 d\Omega_3^2, \quad (8)$$

where the  $X_i$  are expressed in terms of spherical coordinates in the second line. Regarding  $R$  and  $Z$  as functions of  $z$  then yields  $R(z) = e^{\hat{C}}$  and

$$Z(z) = L \int_{\frac{1}{2}}^z \sqrt{e^{2\hat{B}} (1 - (dr_K/dz)^2) - e^{2\hat{C}} (d\hat{C}/dz)^2} dz',$$

where  $\hat{B}$  and  $\hat{C}$  are taken along the curve  $(r_K(z), z)$ , and the length scale  $L$  is reintroduced.

We exhibit surfaces  $Z(R)$  of constant Kretschmann scalar  $K$  for NUBS with deformation  $\lambda = 0.03$  and  $\lambda = 0.47$  in Figs. 4 and 5, respectively.<sup>2</sup> The limit of infinite  $K$  corresponds to the singularity at  $R = 0$ . For UBS, which are also shown,  $R \sim K^{-\frac{1}{8}}$ , independent of  $Z$ . The NUBS surfaces, on the other hand, show an oscillation about constant  $R$  values, and thus a  $Z$  dependence of the power

<sup>2</sup> Note, that close to the horizon the embedding is pseudo-Euclidean with  $dZ^2 \rightarrow -dZ^2$ .

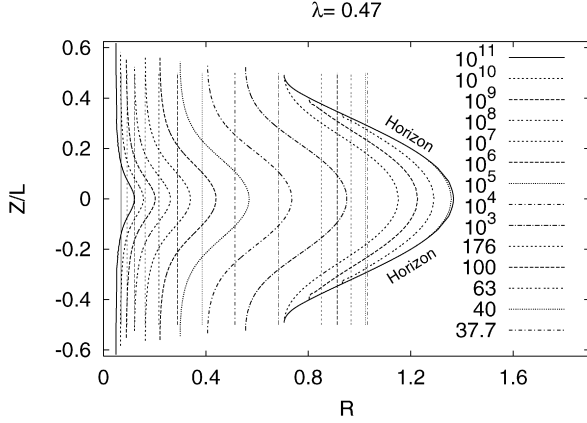


Fig. 5. Same as Fig. 4 for  $\lambda = 0.47$ . The horizon is also shown.

law. Here  $R$  tends more slowly to zero for  $Z = 0$  and faster for  $Z = \pm L_K/2$ , where  $L_K$  denotes the periodic length of  $Z$ . Note, that  $L_K$  increases with increasing  $K$ . Clearly, the deformation of the horizon reflects itself also in the isometric embeddings of the surfaces of constant  $K$ .

In the following we argue that the singularity is space-like for all  $z$ . First we note that for the uniform black string the singularity is space-like, since the spacetime is Schwarzschild  $\times S^1$ . For the nonuniform black strings we consider the worldlines of incoming photons,  $\gamma^\mu = (t(u), r(u), z(u), \theta_1(u), \theta_2(u), \varphi(u))$ , with affine parameter  $u$ . The geodesic equations are obtained as the variational equations of the Lagrangian  $K = g_{\mu\nu} \dot{\gamma}^\mu \dot{\gamma}^\nu$ , where the dot denotes the derivative with respect to  $u$ . Variation with respect to  $t$  yields  $i e^{2\hat{A}} r^2 = k/2 = \text{const.}$ , and the variational equations w.r.t. to the angle coordinates admit solutions  $\theta_1 = \text{const.}$ ,  $\theta_2 = \text{const.}$ ,  $\varphi = \text{const.}$ , due to the symmetries of the non-uniform black string solutions. In this case the remaining variational equations can be cast in the form

$$\frac{d}{du} \left( (\dot{r}^2 - \dot{z}^2) e^{2\hat{B}} - \frac{k^2}{4r^2} e^{-2\hat{A}} \right) = 0, \quad (9)$$

$$\frac{d}{du} (2\dot{r}\dot{z}e^{4\hat{B}}) + \frac{k^2}{4} [\dot{r}\partial_z - \dot{z}\partial_r] \left( \frac{e^{-2(\hat{A}-\hat{B})}}{r^2} \right) = 0. \quad (10)$$

The first equation yields  $\dot{r}^2 - \dot{z}^2 = \frac{k^2}{4r^2} e^{-2(\hat{A}+\hat{B})}$ , consistent with the constraint  $K = 0$  for photons.

We now argue that the direction of the tangential vector  $T^\mu = \frac{d}{du} \gamma^\mu(u)$  is always pointing towards the singularity. We first note that  $e^{-\hat{A}}$ ,  $e^{\hat{B}-\hat{A}}$  and  $e^{-(\hat{A}+\hat{B})}$  tend to zero as the singularity is approached. For incoming null geodesics  $\dot{r} \geq |\dot{z}|$ , where equality holds at the singularity. The ratio of the ‘time’ component to the ‘radial’ component,

$$\frac{\dot{t}}{\dot{r}} = \frac{k}{2r} \frac{e^{-\hat{A}}}{\sqrt{\dot{z}^2 r^2 e^{2\hat{A}} + \frac{k^2}{4} e^{-2\hat{B}}}}, \quad (11)$$

vanishes at the singularity: if  $\dot{z}$  vanishes,  $\dot{t}/\dot{r} = e^{(\hat{B}-\hat{A})}/r$  tends to zero, while for finite  $\dot{z}$ ,  $\dot{t}/\dot{r} \sim e^{-2\hat{A}}/r^2$  also tends to zero.

Thus at the singularity the direction of the tangential vector is  $(0, 1, \pm 1, 0, 0, 0)$ , which points always towards the singularity. Consequently, photons cannot avoid to hit the singularity. The same conclusion holds for massive particles, since their worldlines lie inside the lightcone. Hence the singularity is space-like for all  $z$ .

## 5. Outlook

Concerning the black hole–black string transition we have provided numerical evidence that at the merger point the NUBS singularity touches the horizon at the waist of the strings. What is still missing is the study of the interior of the caged black holes, as they approach the merger point, to see how their curvature and, in particular, their singularity evolve. In  $D = 4$  such a study has been performed recently [15], in higher dimensions, however, this remains a major numerical challenge.

A GL instability arises also for rotating NUBS [16], and a similar instability occurs for asymptotically flat rotating black holes in  $D \geq 6$  dimensions, which have a single angular momentum [17]. This instability then suggests, that as in the case of black strings, a branch of rotating ‘pinched’ (nonuniform) black holes should arise at the marginally stable solution [17]. Exploring this analogy further leads to an intriguing phase diagram for rotating black holes, where horizon topology changing transitions from rotating pinched black holes to black rings, black saturns, and further configurations are expected to occur [18].

## Acknowledgement

We gratefully acknowledge discussions with V. Frolov, E. Radu and A. Shoom. B.K. was supported by the German Aerospace Center.

## References

- [1] B. Kol, Phys. Rep. 422 (2006) 119, hep-th/0411240.
- [2] T. Harmark, V. Niarchos, N.A. Obers, Class. Quantum Grav. 24 (2007) R1, hep-th/0701022.
- [3] H. Kudoh, T. Wiseman, Prog. Theor. Phys. 111 (2004) 475, hep-th/0310104.
- [4] H. Kudoh, T. Wiseman, Phys. Rev. Lett. 94 (2005) 161102, hep-th/0409111.
- [5] R. Gregory, R. Laflamme, Phys. Rev. Lett. 70 (1993) 2837, hep-th/9301052.
- [6] G.T. Horowitz, K. Maeda, Phys. Rev. Lett. 87 (2001) 131301, hep-th/0105111.
- [7] S.S. Gubser, Class. Quantum Grav. 19 (2002) 4825, hep-th/0110193.
- [8] T. Wiseman, Class. Quantum Grav. 20 (2003) 1137, hep-th/0209051.
- [9] E. Sorkin, Phys. Rev. Lett. 93 (2004) 031601, hep-th/0402216.
- [10] B. Kleihaus, J. Kunz, E. Radu, JHEP 0606 (2006) 016, hep-th/0603119.
- [11] B. Kol, JHEP 0510 (2005) 049, hep-th/0206220.
- [12] T. Wiseman, Class. Quantum Grav. 20 (2003) 1177, hep-th/0211028.
- [13] B. Kol, T. Wiseman, Class. Quantum Grav. 20 (2003) 3493, hep-th/0304070.
- [14] G.W. Gibbons, S.W. Hawking, Phys. Rev. D 15 (1977) 2752.
- [15] V.P. Frolov, A.A. Shoom, Phys. Rev. D 76 (2007) 064037, arXiv: 0705.1570 [gr-qc].
- [16] B. Kleihaus, J. Kunz, E. Radu, JHEP 0705 (2007) 058, hep-th/0702053.
- [17] R. Emparan, R.C. Myers, JHEP 0309 (2003) 025, hep-th/0308056.
- [18] R. Emparan, T. Harmark, V. Niarchos, N.A. Obers, M.J. Rodriguez, JHEP 0710 (2007) 110, arXiv: 0708.2181 [hep-th].